Global and Planetary Change 107 (2013) 102–108

Contents lists available at SciVerse ScienceDirect

Global and Planetary Change

journal homepage: www.elsevier.com/locate/gloplacha

Evaluation of aeolian desertification from 1975 to 2010 and its causes in northwest Shanxi Province, China

Zhanjin Xue [a], Zuodong Qin [a,*], Hongjian Li [a], Guangwei Ding [a,b], Xianwen Meng [a]

[a] Institute of Loess Plateau, Shanxi University, No. 92 Wucheng Road, Taiyuan 030006, Shanxi Province, PR China
[b] Chemistry Department, Northern State University, Aberdeen, SD 57401, USA

ARTICLE INFO

Article history:
Received 22 December 2012
Accepted 5 May 2013
Available online 12 May 2013

Keywords:
aeolian desertification
aeolian desertified land (ADL)
desertification causes
northwest Shanxi Province

ABSTRACT

Efforts to control aeolian desertification in China have focused on the arid and semiarid regions. However, the direct dust emission rates, sediment characteristics and local-scale controls, as well as the measures needed to combat desertification, remain poorly understood in northwest Shanxi Province. Aeolian desertification is regarded as an obstacle to local sustainable socioeconomic development. This paper investigated changes in aeolian desertification between 1975 and 2010 on the northwestern Shanxi Plateau. In this study, remote sensing images were used to classify land suffering from aeolian desertification into four categories: light, moderate, severe, and extremely severe. To evaluate the evolution and status of aeolian desertification as well as its causes, we interpreted and analyzed Landsat multi-spectral scanner (MSS) image (acquired in 1975) and Landsat Thematic Mapper (TM) images (acquired in 1991, 2000, 2006, and 2010) as well as meteorological and socioeconomic data. Results revealed 11,866 km^2, 13,362 km^2, 14,051 km^2, 13,613 km^2, and 12,318 km^2 of aeolian desertified land (ADL) in the above 5 periods, respectively. The spatial dynamics and patterns showed two stages: expansion during 1975–2000 at a rate of 87.37 $km^2\ a^{-1}$, and spatial transfer of affected areas during 2000–2010 with a net decrease of 173.27 $km^2\ a^{-1}$. During the evolution of aeolian desertification, areas of moderate ADL had the greatest dynamic response (11.45%). The factors controlling ADL dynamics were analyzed from the perspectives of two groups of factors: natural factors and human activities. Our results indicated that the climate-dominated natural factors contribute greatly to the occurrence and development of ADL. However, they are not the fundamental causes of its development. The human factors are the primary and direct driving forces responsible for the increase in ADL area. More thorough quantitative analysis, with more frequent remotely sensed data is needed to assess the driving forces in more detail.

1. Introduction

Desertification, defined by the United Nations Convention to Combat Desertification (UNCCD) as "land degradation in the arid, semi-arid, and dry sub-humid areas resulting from various factors, including climatic variations and human activities", is a serious global environmental and ecological issue (Abubakar, 1997; Warren, 2002; Singh, 2009; Verstraetel et al., 2009; Andrew, 2010; Dawelbait and Morari, 2012; D'Odorico et al., 2013). Globally desertified land amounts to 3.6×10^7 km^2, covers 24.1% of Earth's land surface, and affects about one-sixth of the world's population, many of whom live in poverty (Middleton and Thomas, 1997).

Combating desertification is crucial to the reduction of global poverty, and involves understanding the causes and feedbacks (Sivakumar, 2007; Barbero-Sierra et al., 2013; Salvati et al., 2013), monitoring and assessing the progression (Helldén, 2008; Helldén and Topptrup, 2008; Ladisa et al., 2012), and designing and implementing site-specific management strategies (D'Odorico et al., 2013). In recent years, the notion of desertification has been related to losses of ecosystem services resulting from the effect of anthropogenic disturbances and/or climate variations in dryland ecosystems (D'Odorico et al., 2013).

Aeolian desertification is the most serious eco-environmental problem in northern China, where the area of aeolian desertified land (ADL) totals 1.839 million km^2 and is distributed across 13 provinces in northwest, north, and northeast China (CCICCD, 2006). During the past 60 years, ADL has increased rapidly at rates of 1560 $km^2\ a^{-1}$ in the 1950s, 2100 $km^2\ a^{-1}$ in the 1970s, 2460 $km^2\ a^{-1}$ in the 1980s, and 3436 $km^2\ a^{-1}$ in the 1990s (CCICCD, 2002). The direct economic loss caused by aeolian desertification was about 54.1 billion RMB Yuan a^{-1} (Zhang et al., 1996). In recent years, aeolian desertification in northern China has attracted worldwide concern. Many studies have investigated the process of aeolian desertification and its impacts on the environment (Zhu and Li, 2002; Xue et al., 2009; Guo et al., 2010; Hu et al., 2012). The most common outcomes have related desertification not only to climate-related changes, but also to human-induced impacts, and especially those associated with inappropriate land use, agricultural

* Corresponding author. Tel./fax: +86 351 701 0700.
E-mail address: qzd3097@sina.com.cn (Z. Qin).

0921-8181/$ – see front matter.
http://dx.doi.org/10.1016/j.gloplacha.2013.05.001

intensification, and woodland consumption (Zhao et al., 1999; Zhang et al., 2008; Shen et al., 2012; Wang et al., 2012).

Northwest Shanxi is located between the agriculture and animal husbandry ecotones in northern China, and is situated in West and up-wind of Beijing–Tianjin. As well as being an important part of Loess Plateau and the "golden triangle" of Shanxi–Shaanxi–Inner Mongolia, the Chinese government listed it in "The Second Phase of Beijing–Tianjin Sand Source-Control Program (2013–2022)" in 2012. Aeolian desertification has strongly inhibited the sustainable socio-economic development of northwest Shanxi, and adversely affected the ecological security of Beijing–Tianjin and the energy security in China. Since 1990s, rich coal and iron resources have been exploited in this region, the study of aeolian desertification is a sensitive topic due to the conflict between combating aeolian desertification and resource exploration. Recently, researchers studied the status, types, and/or harmfulness of aeolian desertification in northwest Shanxi (Qin, 1996; Ma and Su, 2003; Xue and Qin, 2012). However, these studies lacked long-time aeolian desertification monitoring and an integrated cause analysis to explore the mechanisms contributing to aeolian desertification. Moreover, spatial patterns of changes and the dynamic characteristics of aeolian desertification have not been reported in previous investigations.

The main objectives of this study were to understand the area of ADL, its distribution, and spatio-temporal dynamics in the region from 1975 to 2010 using remote sensing (RS) data and geographic information system (GIS), and then integrate cause analysis: natural factors and human activities. Through this study, we explored the occurring mechanism of aeolian desertification. This result will be important in supporting better-informed decisions and in developing more effective policies to combat aeolian desertification in northwest Shanxi.

2. Study area

Northwest Shanxi lies between longitudes 111°19′E and 112°52′E, and between latitudes 38°39′N and 40°17′N. It covers an area of about 1.42×10^4 km^2 and includes nine counties (Zuoyun, Youyu, Pinglu, Shuocheng, Hequ, Pianguan, Baode, Shenchi, and Wuzhai) (Fig. 1). It is surrounded by the Yellow River to the west, the Datong Basin to the east, the Luya Mountains to the south, and the Great Wall to the north. The landscape in the study area is gently undulating, with an average elevation of 1300–1500 m. Several rivers, such as the Cangtou, Pianguan, Zhujiachuan, Yuanzi, and Hui flow through the area. The region lies in the transitional zones from semi-humid to semi-arid climate and from shrub steppe to meadow vegetation (Qin, 1996). The study area is characterized by dry and cold winters, arid and windy springs. It has a wide temperature difference between summer and winter. Mean annual air temperature was between 3.6 °C and 7.5 °C, with monthly mean temperatures of −16.0 to −10.0 °C in January and 19.0–22.5 °C in July. The average annual precipitation ranged from 400 mm in the north to 500 mm in the south, of which 75–80% occurs during June–September. The average annual evaporation ranged between 1780 mm and 1950 mm, increasing from south to north; and was four times greater than the precipitation. The mean annual wind speed was more than 4.0 m s^{-1}, and the mean number of gale days was more than 20 days. Wind speeds could reach 17–21 m s^{-1}, usually in the period from March to May. The main vegetation types were secondary scrub and grasses, where the dominant species were *Hippophae rhamnoides*, *Caragana korshinskii*, *Ostryopsis davidiana*, *Rosa xanthina*, *Bothriochloa ischaemum*, and *Artemisia*. The main soil types in this region were Orthic Entisols, Sandic Entisols, and Orthic Anthrosols. Therefore, the coincidence of windy weather and low vegetation cover in winter and spring, and abundant sandy material, were the fundamental

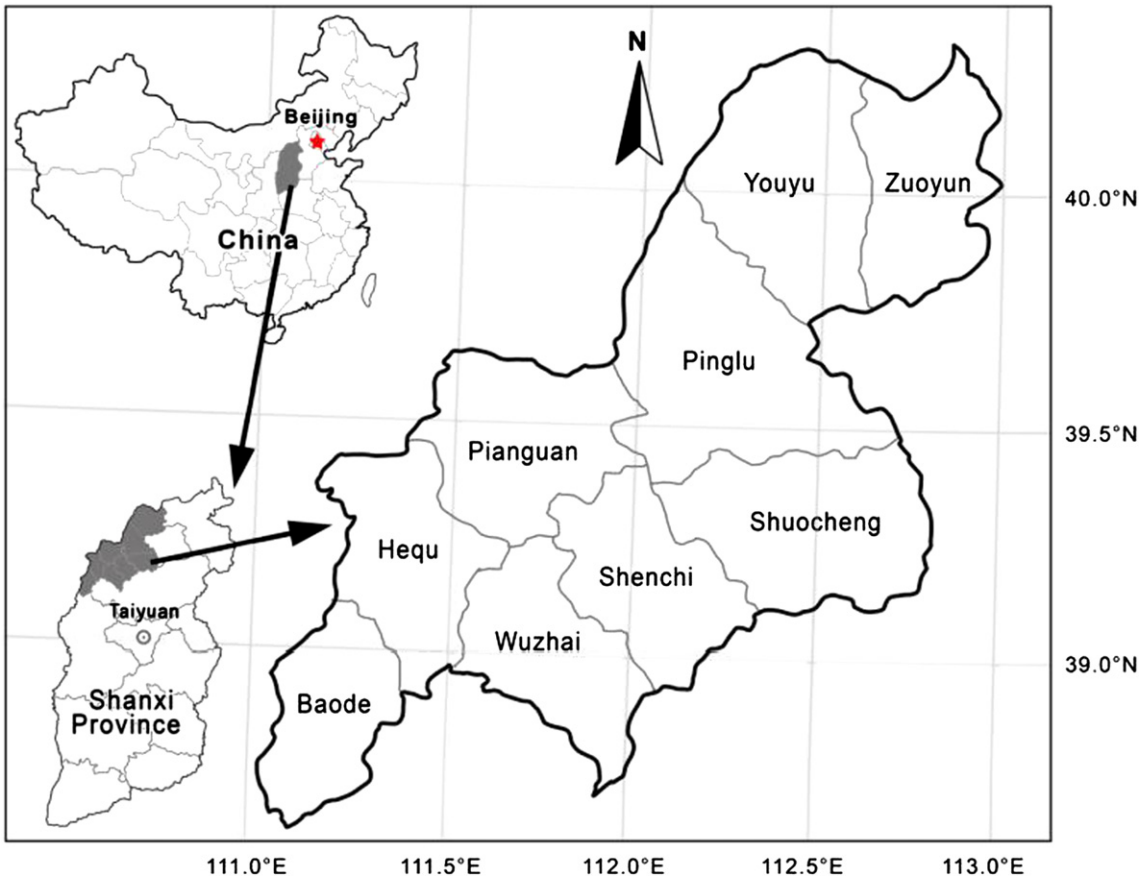

Fig. 1. Location of the study area.

environmental conditions for aeolian desertification occurrence in northwest Shanxi.

3. Materials and methods

3.1. Classification system for aeolian desertification

Dispersed, patchy vegetation cover, and sand sheets were the main landscape characteristics of ADL. These were the visual indicators of environmental changes and the severity of desertification (Diouf and Lambin, 2001). After reviewing the classification criteria proposed in previous studies (Zhu and Liu, 1984; Wu, 2001; Sun et al., 2008; Yan et al., 2009; Guo et al., 2010; Shen et al., 2012; Wang et al., 2012), we chose the proportions of the total area covered by shifting sand and vegetation coverage as the main criteria for deriving the desertification status used in this study. We divided desertification intensity into four grades based on the relative areas of shifting sand and vegetation coverage: light, moderate, severe, and extremely severe (Table 1).

3.2. Data acquisition, processing, and analysis

Remote sensing (RS) data are valuable sources for extracting spatially and temporally explicit information (Corbane et al., 2008; Helldén and Topptrup, 2008). In particular, multispectral satellite imagery, such as these provided by Landsat MSS, TM, and ETM images, is a precious resource for long-term analysis of surface processes, *e.g.*, changes in landforms and land degradation, at a regional scale (Alatorre and Beguería, 2009; Liberti et al., 2009). To assess the evolution of aeolian desertification in northwest Shanxi, we employed MSS image in 1975, and TM images from the four dates (1991, 2000, 2006, and 2010), with a spatial resolution of 80-m (MSS) and 30-m (TM). The MSS image was obtained from Shanxi Center of Geographical Information, and the TM images were obtained from the International Scientific Data Service Platform (http://datamirror.csdb.cn/). All images recorded between June and September were selected because ADL was more easily recognized during this period of maximum vegetation growth (Hu et al., 2012). Landsat images were utilized because they had high quality temporal resolution and covered areas appropriate for monitoring the environment in a large geographical zone.

False-color image extraction by stacking near-infrared, red and green bands, as well as geometrical correction, was carried out using Erdas Imagine 8.7 software provided by ERDAS. Image was accurate to within one pixel. Details of the satellite image processing method were described by Valle et al. (1998) and Vasconcelos et al. (2002). We were confident that this technique was applied effectively in our study. The evaluation of aeolian desertification included not only the total area of ADL but also the extent of degradation (Liu and Wang, 2007). Field surveys were carried out to relate image features to actual ADL grades during ground-truthing immediately after all images acquisition. The ADL grades were identified at each survey location according to the classification criteria. Survey locations were measured by global positioning system, and land surface features were recorded by digital camera. Resulting image features corresponding to different grades of ADL are listed in Table 1. All images were interpreted manually using ARCGIS 9.1, following the classification criteria (Table 1). In order to confirm the reliability of interpreted results, a second field survey was conducted in September 2011 to resolve uncertain areas. Subsequent corrections were made after the field validation to ensure classification accuracy over 95%. Finally, statistical data and spatial distribution maps of ADL were obtained by ARCGIS 9.1 and were used to analyze temporal changes and the spatial patterns and dynamics of aeolian desertification, and to reconstruct the development and evolution of aeolian desertification throughout the study period. To detect transfer between different grades of ADL, the graphical superposition method introduced by Li et al. (2007) was employed to establish the ADL transfer matrix.

Formula (1) below was used to illustrate the dynamic response of aeolian desertification in other arid and semi-arid regions in the north of China (Zhao et al., 2001; Li et al., 2004; Guo et al., 2010).

$$AD_k = AT_k \div AI_k \times 1/T \times 100\% \quad (1)$$

where k is the grade of aeolian desertification, representing light, moderate, severe, and/or extremely severe aeolian desertification; AD_k is the dynamic response of aeolian desertification of grade k; AI_k is the area of the kth grade of aeolian desertification in the initial year of a study period; AT_k is the area of the kth grade of aeolian desertification, which was transferred to other grades of aeolian desertification or non-aeolian desertification during the study period; and T is the duration of the study period.

3.3. Meteorological and socioeconomic data collection

Local meteorological and socioeconomic data were collected and analyzed to explore the mechanism and processes of aeolian desertification. The meteorological data were collected from five meteorological stations (Zuoyun, Shuocheng, Pianguan, Wuzhai, and Baode) in the form of monthly observed values for temperature, precipitation, and gale days from 1975 to 2010. We acquired annual values by summing the monthly values (precipitation and gale days) or by averaging the monthly values (temperature). As proxies of human activity between 1975 and 2010, we chose the population in each year, livestock numbers (cattle, horses, goats, and sheep), and forest coverage. We collected the data from the statistics departments of local governments and Shanxi Provincial Bureau of Statistics. Thematic maps, including geomorphologic maps, vegetation maps, and land use maps, were also used as supplementary data sources.

Table 1
Classification and indicators of aeolian desertification grades.

Grade of aeolian desertification	Shifting sand (%)	Vegetation coverage (%)	Land surface characteristics	Tone and texture of RS images
Light	<5	>60	Blowout appears on windward slope of sand dunes and shifting sand is speckled. Vegetation has suffered from degradation in some areas.	Light red, dotted by darker red; coarse and partially bare surface.
Moderate	5–25	30–60	Shifting sand appears on windward slopes of shrub sand dunes and flats between sand dunes, the vegetation cover is significant but is interspersed with sand sheets or wind-eroded areas.	Irregular blocks, and the shapes of sand dunes are clear.
Severe	25–50	10–30	Sand dunes are in a half-shifting state, there is sparse vegetation cover.	Irregular brownish yellow or yellow white surface, dotted shrubs can be identified. Image surface is rough.
Extremely	>50	<10	Sand dunes in a shifting state, there is little or no vegetation.	Yellow or white surface, incanus, shifting sand dunes or sand ridges can be identified. There is wavy texture feature.

Table 2
Dynamics of ADL during the study period.

Years	Light		Moderate		Severe		Extremely severe		Total	
	Area/km^2	% of ADL	Area/km^2	% of ADL	Area/km^2	% of ADL	Area/km^2	% of ADL	Area/km^2	% of total area
1975	11,865.64	99.97	1.03	0.02	0.20	0.01	0	0	11,866.87	83.57
1991	13,357.23	99.96	3.15	0.03	1.59	0.01	0	0	13,361.97	94.10
2000	2552.40	18.16	11,462.30	81.58	34.71	0.25	1.65	0.01	14,051.06	98.95
2006	11,566.49	84.96	2039.11	14.98	6.29	0.04	0.91	0.02	13,612.80	95.86
2010	12,124.66	98.42	187.26	1.52	5.70	0.04	0.71	0.02	12,318.33	86.75

4. Results

4.1. Dynamic changes in ADL since 1975

Analyzing dynamic changes in desertification can help to reveal the mechanisms responsible for desertification development and the relationships between the driving forces and the resulting changes (Wang et al., 2012). The data in Table 2 indicated that ADL in northwest Shanxi continually expanded until 2000 and was gradually rehabilitated during 2000–2010. From 1975 to 2000, ADL reached its largest area of 14,051.06 km^2, at a rate of increase of 87.37 km^2 a^{-1}. After 2000, ADL totaled 13,612.80 km^2 in 2006 and 12,318.33 km^2 in 2010, decreasing at a rate of 73.04 km^2 a^{-1} and 323.62 km^2 a^{-1} during 2000–2006 and 2006–2010, respectively. The data further showed that the areas of moderate, severe, and extremely severe ADL classes increased before 2000 and decreased after 2000. Two other processes affecting aeolian desertification were recognized in the satellite image data set. The first one was related to sand exposure. In the northern part of the study area, a sand dune stabilized by natural vegetation was visible in the TM image. However, subsequent deforestation for domestic purposes and overgrazing caused degradation of the site.

4.2. Spatial changes, and transfer between different grades of ADL

In 1975, the ADL was concentrated in the middle of the region (Fig. 2), mainly in Youyu, Pinglu, Shuocheng, and Pianguan. Light ADL was the primary type, with an area of 11,865.64 km^2 accounting for 99.97% of the total area of ADL (Table 2). From 1975 to 1991, ADL began to enlarge. Fig. 2 clearly indicated that ADL was covered in the north of the region. Although extremely severe ADL had not changed, the light ADL increased 1491.59 km^2 (Table 2); and 1506.12 km^2 of non-ADL was transferred into light ADL (Table 3), which mainly appeared in Zuoyun and Youyu. Since 1978, an unprecedented combination of economic reforms, exploration for natural resources, and population growth has led to a dramatic transformation of land cover in the study area. During these changes, the area of ADL has increased as a result of excessive land reclamation for agriculture and other human activities.

In 2000, the magnitude of desertification ranged from low to extreme, with a prevalence of severe degradation conditions (high or extreme). Analysis of changes also demonstrated the existence of re-growth conditions, mostly distributed in the south-eastern areas (Pianguan, Hequ, Baode, and Wuzhai) (Fig. 2). Overall, desertification

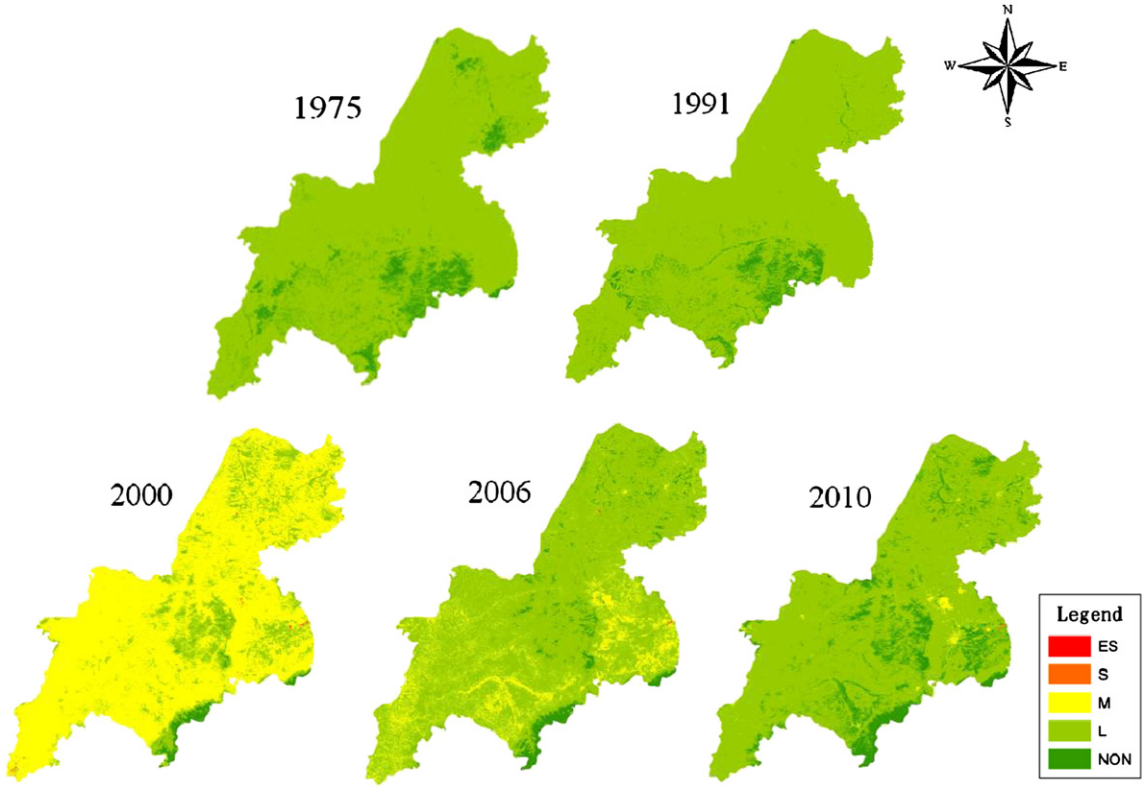

Fig. 2. Spatial distribution of various grades of ADL in northwest Shanxi. L — land with light aeolian desertification, M — land with moderate aeolian desertification, S — land with severe aeolian desertification, ES — land with extremely severe aeolian desertification, and NON — with non-aeolian desertified land.

Table 3
Transfer matrix of different grades of ADL (abbreviations follow Fig. 2).

Transferred area (km^2)						
Year	Grades	L	M	S	ES	NON
1975–1991	L	11,851.07	2.42	0.92	0	11.23
	M	0.04	0.51	0.46	0	0.02
	S	0	0.02	0.18	0	0
	ES	0	0	0	0	0
	NON	1506.12	0.20	0.03	0	
Total	Newly aeolian desertified: 1506.35				Rehabilitated: 11.25	
1991–2000	L	2208.46	11,098.72	28.77	1.35	19.93
	M	0.44	1.35	0.35	0.27	0.74
	S	0.20	0.10	0.76	0.03	0.50
	ES	0	0	0	0	0
	NON	343.30	362.13	4.83	0	
Total	Newly aeolian desertified: 710.26				Rehabilitated: 21.17	
2000–2006	L	1846.16	287.28	0.20	0.04	418.72
	M	9553.17	1646.39	0.40	0.11	262.23
	S	9.83	16.16	5.14	0.12	3.46
	ES	0.08	0.41	0.51	0.62	0.03
	NON	157.25	88.87	0.04	0.02	
Total	Newly aeolian desertified: 246.18				Rehabilitated: 684.44	
2006–2010	L	10,638.15	35.29	0	0	893.05
	M	1448.41	132.46	0.27	0	457.97
	S	0.32	0.60	5.24	0.06	0.07
	ES	0	0.07	0.19	0.65	0
	NON	37.78	18.84	0	0	
Total	Newly aeolian desertified: 56.62				Rehabilitated: 1351.09	

prevailed over re-growth. As a result, moderate ADL had the largest area of 11,462.30 km^2, accounting for 81.58% of the total area in 2000 (Table 2). Some 362.13 km^2 of non-ADL was transferred into moderate ADL (Table 3). However, these averages were not sufficient to provide a clear indication of the driving factors of change at the landscape scale.

The ADL in 2006 had decreased relative to that in 2000. Fig. 2 demonstrated that ADL appeared in the south of this region, such as in Hequ, Baode, Wuzhai, and Shuocheng. It was possible that over-exploitation of semi-desert environments through deforestation, overgrazing, and cultivation resulted in habitat conversion to desert, even though rainfall may still have been sufficient to support semi-desert vegetation. However, ADL in the north of this region had become largely rehabilitated. According to Table 3, there were 246.18 km^2 of new ADL, while 684.44 km^2 had been rehabilitated. Re-growth conditions observed in the north of the region were mainly due to government reforestation projects in the last decade and sustained favorable conditions for vegetation growth in the study area.

In 2010, more ADL was rehabilitated in the south, mainly in Hequ, Baode, and Wuzhai (Fig. 2). During 2006–2010, 56.62 km^2 of non-ADL was desertified and 1351.09 km^2 was rehabilitated. Meanwhile, 893.05 km^2 of light ADL was rehabilitated and 37.78 km^2 of non-ADL became light ADL, accounting for 66.73% and 66.10% of the new rehabilitation and desertification, respectively (Table 3). Light ADL reached an area of 12,124.66 km^2, or 98.42% of the total ADL.

4.3. Characterization of dynamic response for different grades of ADL

We described the dynamic response of aeolian desertification by function (1). Dynamic response was calculated for four periods, and results are listed in Table 4. In general, less severe aeolian desertification grades had a greater dynamic response (Guo et al., 2010). However, in our study, the moderate grade showed the greatest dynamic response: 13.70% and 23.38% during 2000–2006 and 2006–2010, respectively. This might be caused by the comparatively small area of moderate ADL in 1975 and 1991 (Table 2). Noticeably, light aeolian

Table 4
Dynamic response of ADL for different periods.

Dynamic response (%)					
Grades	1975–1991	1991–2000	2000–2006	2006–2010	Average
Light	0.01	8.34	4.43	2.01	3.70
Moderate	3.03	5.71	13.70	23.38	11.45
Severe	0.60	5.22	13.63	4.17	5.91
Extremely severe	0	0	9.99	7.14	4.28

desertification had the lowest dynamic response in the study period, and its average value of 3.70% was less than one third of the highest average value of 11.45% (Table 4). This may suggests that light ADL could rarely be rehabilitated.

5. Discussion

Natural factors and human factors were the two major driving forces of aeolian desertification processes in the region, and could both influence aeolian desertification at the level of regional landscapes (Avni et al., 2006; Seifan, 2009; Yan et al., 2009; Dawelbait and Morari, 2012). Traditional digital remote sensing analysis was based on the consideration that a pixel was uniformly covered. Therefore, classification techniques assigned each pixel to just one single category. In most environmental applications, this homogeneity was unusual; and normally the area included in the instantaneous field of view of a satellite sensor was a composite of several land covers: for example, grass, trees, shrubs, soils or man-made features. For aeolian desertification studies this heterogeneity was especially critical, since semi-arid areas were commonly a combination of vegetation and soil in different proportions.

5.1. Natural factors

5.1.1. Material factor

Abundant sandy material was one of the prerequisites for the occurrence of aeolian desertification (Hu et al., 2012). The terrain in the study area was Loess hills with cladding sand in northwest Shanxi. Loose Quaternary sediments were deposited on the hillsides and terraces. The mechanical composition of surface material was predominantly extremely fine sand (0.063–0.125 mm) and fine sand (0.125–0.250 mm) (Ma and Su, 2003). The clay fraction (<0.002 mm) was under 20%. The mainly sandy soil and lack of binding or viscous substances provided an abundant source of sand for aeolian desertification.

5.1.2. Climate factor

Climate was an important driving force for aeolian desertification (Zhu and Liu, 1984). Climate affects aeolian desertification mainly through the influence of changes in air temperature, precipitation, and wind velocity (Lancaster and Helm, 2000; Wang et al., 2009). In this study, air temperature, precipitation, and wind velocity data were collected to analyze climatic changes during the study period. We used a linear regression model to define the trends in mean annual temperature and total precipitation. The mean annual temperature increase per decade was 0.22 °C (1975–1990), 0.24 °C (1991–2000), and 0.21 °C (2001–2010) in the study area (Fig. 3), which was much greater than the global mean rate of increase (0.03–0.06 °C per decade) (Hu et al., 2012). Increased air temperature could result in increasing topsoil evaporation and decreasing topsoil moisture content, which intensified vegetation degradation and wind erosion (Xue et al., 2009). Meanwhile, the data in Fig. 3 demonstrated that the mean annual precipitation fluctuated slowly, but without a significant decreasing or increasing tendency throughout the study period. The wind in the region was strong, according to the observed data from 1975 to 2010. The mean annual number of gale days (wind speed of 17–21 m s^{-1}) per decade was 25.7 (1975–1990), 26.5

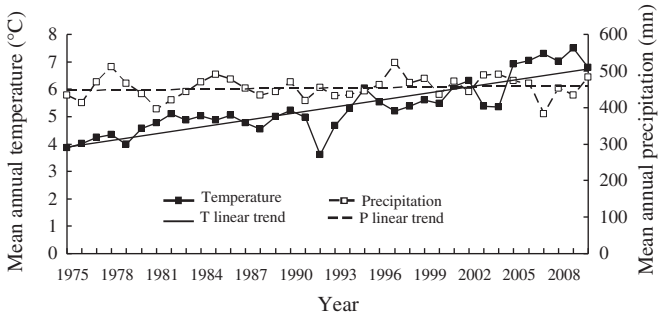

Fig. 3. Changes in annual temperature and precipitation since 1975.

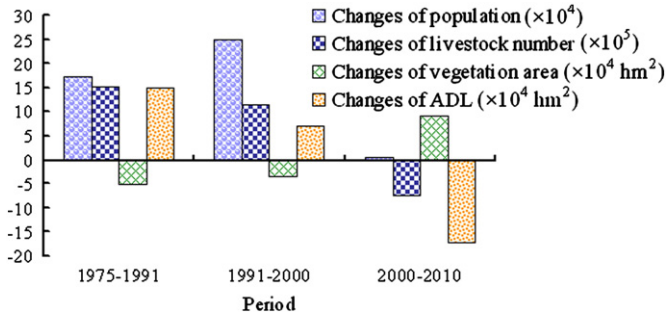

Fig. 5. Comparison of ADL in three periods relative to the proxies of human activities in northwest Shanxi.

(1991–2000), and 24.2 days (2001–2010) (Fig. 4), respectively, which occurred from March to May before the rainy season arrives. An observed cubic relationship between the wind's erosive power and wind velocity (Yan et al., 2009) suggested the influence of wind on aeolian desertification was stronger than temperature and precipitation in the study period.

Higher temperatures could cause more evaporation, and thus, more arid conditions (Wang et al., 2005). During our study period, the overall aridity of the climate increased because temperatures had steadily increased while precipitation had not obviously changed throughout the study area (Fig. 3). The combined effect of changes in temperature, precipitation, and wind should has worsened aeolian desertification from 1975 to 2010; and indeed, aeolian desertification increased during 1975–2000. However, in 2000–2010 aeolian desertification showed net rehabilitation. Therefore, the climate-dominated natural factors were not the main driving forces for the development of aeolian desertification in northwest Shanxi.

5.2. Human factor

Natural factors such as climatic variations created the potential for the development of aeolian desertification. However, human activities appeared to be the most important factors responsible for the initiation of aeolian desertification (Ma et al., 2007; Guo et al., 2010; Wang et al., 2012). In the present study, we evaluated human activities using three proxies: the human population, the number of livestock, and forest coverage. Our results illustrated that there had been significant variations in these proxies throughout the study period in northwest Shanxi (Fig. 5).

The region's population increased by 17.5×10^4 (from 149.5×10^4 to 167×10^4) and 25×10^4 (from 167×10^4 to 192×10^4) during 1975–1991 and 1991–2000 (Fig. 5), respectively, which increased the need for farmland, and the resulting conversion of grasslands and woodlands to agricultural uses led to degradation or destabilization. Due to a lack of adequate surface protection, the soil either became eroded or the reclaimed land was subsequently invaded and covered by windblown sand. During 2000–2010, the population showed no obvious changes, and under the Migrating Policy 6.50×10^4 people migrated to engage in non-agricultural activities, which greatly alleviated the pressure on the land.

In two former periods, the number of livestock increased by 15.26×10^5 (from 19.02×10^5 to 34.28×10^5) and 11.43×10^5 (from 34.28×10^5 to 45.71×10^5) (Fig. 5), of which 85% of livestock was free-herding. According to our investigation, the number density of sheep grazing was 150% greater than the bearing capacity of grassland. 'Over-grazing' resulted in a serious degradation of grassland, such as the quality of edible herbs deteriorated while the abundance of toxic herbs increased. Meanwhile, due to trampling, the top layer of the soil surface had been destroyed and lost its ability to hold moisture, resulting in increased evaporation and surface run-off, and altering soil–water–plant relationships and exposing bare soil to erosion. From 2000 to 2010, the number of livestock had reduced by 7.36×10^5 from 45.71×10^5 to 38.35×10^5 (Fig. 5), and 65% of livestock was trap-herding because of the Prohibiting Grazing Policy (Xue and Qin, 2012). The deserted grassland began to rehabilitate.

Despite ample coal resources, local inhabitants were poor because of living in a poverty-stricken area where they had to cut natural shrubs and/or trees for firewood. Consequently, 'over-cutting' resulted in the loss of 8.65×10^4 hm^2 natural shrubs and/or trees during 1975–2000, and reduced forest coverage to less than 11% of the whole region in 2000. Therefore, the semi-fixed and fixed sandy land was re-activated into mobile sandy land by strong wind erosion in the area. In the latter ten years, the Chinese government implemented many programs to protect arid or semiarid regions from aeolian desertification, such as "Three-North" Shelterbelt Project, Conversion of Cropland to Forest or Grassland Program, Water and Soil Conservation Program and others (Xue and Qin, 2012). Under these programs, the forest coverage increased from 10.25% (14.55×10^4 hm^2) in 2000 to 16.69% (23.70×10^4 hm^2) in 2010 in northwest Shanxi (Fig. 5), with Youyu County reaching a notable 31.44% in 2010.

In our study area, the expansion or rehabilitation of ADL followed the increase or decrease of population, livestock, and forest coverage during the 1975–2010 periods (Fig. 5). Therefore, we found that human factors were the main contributors and the fundamental causes of the process of aeolian desertification.

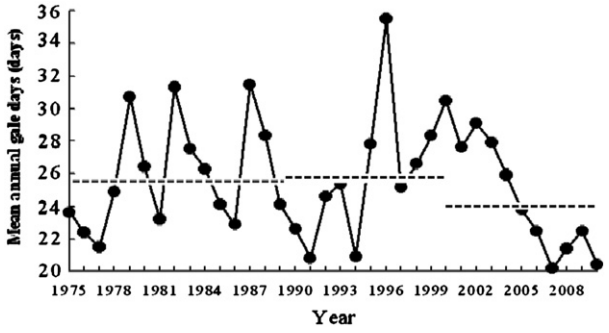

Fig. 4. Changes in annual gale days (those exceeding Force 8) since 1975.

6. Conclusion

The ADL expanded from 1975 to 2000 at a rate of 87.37 km^2 a^{-1}, and was rehabilitated after 2000 at a rate of 173.27 km^2 a^{-1}, according to results obtained from remote sensing (MSS, TM) image analysis coupled with field surveying in northwest Shanxi. During the evolution of aeolian desertification, the moderate ADL class had the greatest dynamic response (11.45%). Both natural and human factors contributed to the deterioration of aeolian desertification conditions in the study period. The natural factors (such as the warming and windy climate, and abundant surface sand source) were the

prerequisite for the region's potential aeolian erosive activities. However, the human factors such as population growth, overgrazing, and over-cutting were the external driving forces that were mainly and directly responsible for the increase of ADL.

Despite our promising results in this study, there were limitations to the accuracy of aeolian desertification monitoring using Landsat data. For example, we may have the ability to acquire high-quality images but lack experienced visual interpreters. In future research, we plan to collect more efficient and objective data and develop a more effective quantitative method to evaluate aeolian desertification and its human factor in northwest Shanxi.

Acknowledgments

This research was supported by the International Science & Technology Cooperation Program of China (2012DFA20770), Science and Technology Major Project of Shanxi Province (20121101011), and National Nature Science Foundation of China (41101013, 41201043). We thank Dr. Bao Yang and two reviewers for their constructive comments to improve the manuscript greatly.

References

Abubakar, S.M., 1997. Monitoring land degradation in the semiarid tropics using an inferential approach: the Kabomo Basin case study, Nigeria. Land Degradation & Development 8, 311–323.
Alatorre, L., Beguería, S., 2009. Identification of eroded areas using remote sensing in a badlands landscape on marls in the central Spanish Pyrenees. Catena 76 (3), 182–190.
Andrew, W., 2010. Sustainability in aeolian systems. Aeolian Research 1, 95–99.
Avni, Y., Porat, N., Plakht, J., Avni, G., 2006. Geomorphic changes leading to natural desertification versus anthropogenic land conservation in an arid environment, the Negev Highlands, Israel. Geomorphology 82, 177–200.
Barbero-Sierra, C., Marques, M.J., Ruíz-Pérez, M., 2013. The case of urban sprawl in Spain as an active and irreversible driving force for desertification. Journal of Arid Environments 90, 95–102.
CCICCD, 2002. China National Report on the Implementation of the United Nation's Convention to Combat Desertification.
CCICCD, 2006. China National Report on the Implementation of the United Nation's Convention to Combat Desertification.
Corbane, C., Raclot, D., Jacob, F., Albergel, J., Andrieux, P., 2008. Remote sensing of soil surface characteristics from a multiscale classification approach. Catena 75 (3), 308–318.
D'Odorico, P., Bhattachan, A., Davis, K.F., Ravi, S., Runyan, C.W., 2013. Global desertification: drivers and feedbacks. Advances in Water Resources 51, 326–344.
Dawelbait, M., Morari, F., 2012. Monitoring desertification in a Savannah region in Sudan using Landsat images and spectral mixture analysis. Journal of Arid Environments 80, 45–55.
Diouf, A., Lambin, E.F., 2001. Monitoring land-cover changes in semi-arid regions: remote sensing data and field observations in the Ferlo, Senegal. Journal of Arid Environments 48 (2), 129–148.
Guo, J., Wang, T., Xue, X., Ma, S.X., Peng, F., 2010. Monitoring aeolian desertification process in Hulunbir grassland during 1975–2006, Northern China. Environmental Monitoring and Assessment 166, 563–571.
Helldén, U., 2008. A coupled human-environment model for desertification simulation and impact studies. Global and Planetary Change 64, 158–168.
Helldén, U., Topptrup, C., 2008. Regional desertification: a global synthesis. Global and Planetary Change 64, 169–176.
Hu, G.Y., Dong, Z.B., Lu, J.F., Yan, C.Z., 2012. Driving forces responsible for aeolian desertification in the source region of the Yangtze River from 1975 to 2005. Environmental Earth Sciences 66, 257–263.
Ladisa, G., Todorovic, M., Trisorio, Liuzzi G., 2012. A GIS-based approach for desertification risk assessment in Apulia region, SE Italy. Physics and Chemistry of the Earth 49, 103–113.
Lancaster, N., Helm, P., 2000. A test of a climatic index of dune mobility using measurements from the southwestern United States. Earth Surface Processes and Landforms 25, 197–208.
Li, F., He, Y.F., Liu, Z.M., Zhang, B., 2004. Dynamics of sandy desertification and its driving forces in western Jilin province. Chinese Geographical Science 14 (1), 57–62.
Li, S., Zheng, Y., Luo, P., Wang, X., 2007. Desertification in western Hainan Island, China (1959 to 2003). Land Degradation & Development 18, 473–485.
Liberti, M., Simoniello, T., Carone, M.T., Coppola, R., D'Emilio, M., Macchiato, M., 2009. Mapping badland areas using LANDSAT TM/ETM satellite imagery and morphological data. Geomorphology 106 (3–4), 333–343.
Liu, S.L., Wang, T., 2007. Aeolian desertification from the mid-1970s to 2005 in Otindag Sandy Land, Northern China. Environmental Geology 51, 1057–1064.
Ma, Y.J., Su, Z.Z., 2003. Study on sandy desertification of present situation and developmental trend in Shanxi Province. Journal of Soil and Water Conservation 17, 81–84.
Ma, Y.H., Fan, S.Y., Zhou, L.H., Dong, Z.Y., Zhang, K.C., Feng, J.M., 2007. The temporal change of driving factors during the course of land desertification in arid region of North China: the case of Minqin County. Environmental Geology 51, 999–1008.
Middleton, N., Thomas, D.S.G., 1997. World Atlas of Desertification. Arnold 182.
Qin, Z.D., 1996. Study on the evaluation of land desertification harmfulness in the Northwestern part of Shanxi Province. Arid Land Geography 19, 8–15.
Salvati, L., Sateriano, A., Zitti, M., 2013. Long-term land cover changes and climate variations—a country-scale approach for a new policy target. Land Use Policy 30, 401–407.
Seifan, M., 2009. Long-term effects of anthropogenic activities on semi-arid sand dunes. Journal of Arid Environments 73, 332–337.
Shen, W.S., Li, H.D., Sun, M., Jiang, J., 2012. Dynamics of aeolian sandy land in the Yarlung Zangbo River basin of Tibet, China from 1975 to 2008. Global and Planetary Change 86–87, 37–44.
Singh, G., 2009. Salinity-related desertification and management strategies: Indian experience. Land Degradation & Development 20, 367–385.
Sivakumar, M.V.K., 2007. Interactions between climate and desertification. Agricultural and Forest Meteorology 142, 143–155.
Sun, Y.J., Zhou, Q., Yang, R.H., 2008. A study of land desertification dynamic change in Yellow River basin. Remote Sensing for Land and Resources 76 (2), 74–78.
Valle, H.F., Elissalde, N.O., Gagliardini, D.A., Milovich, J., 1998. Status of desertification in the Patagonian Region: assessing and mapping from satellite imagery. Arid Soil Research and Rehabilitation 12, 95–122.
Vasconcelos, M., Mussa-Biai, J.C., Araujo, A., Diniz, M.A., 2002. Land cover changes in two protected areas of Guinea-Bissau (1956–1998). Applied Geography (Sevenoaks, England) 22, 139–156.
Verstraetel, M.M., Scholes, R.J., Smith, M.S., 2009. Climate and desertification: looking at an old problem through new lenses. Frontiers in Ecology and the Environment 7, 421–428.
Wang, X., Chen, F.H., Dong, Z., Xia, D., 2005. Evolution of the southern Mu US Desert in north China over the past 50 years: an analysis using proxies of human activity and climate parameters. Land Degradation & Development 16, 351–366.
Wang, X.M., Yi, Y.C., Dong, Z.B., Zhang, C.X., 2009. Responses of dune activity and sandy land in China to global warming in the twenty-first century. Global and Planetary Change 67, 167–185.
Wang, T., Yan, C.Z., Song, X., Xie, J.L., 2012. Monitoring recent trends in the area of aeolian desertified land using Landsat images in China's Xinjiang region. ISPRS Journal of Photogrammetry and Remote Sensing 68, 184–190.
Warren, A., 2002. Land degradation is contextual. Land Degradation & Development 13, 449–459.
Wu, W., 2001. Using the TM image for monitoring land desertification. Remote Sensing Technology and Application 16, 86–90.
Xue, Z.J., Qin, Z.D., 2012. Economic loss of aeolian desertification in north Shanxi province. Journal of Arid Land Resources and Environment 4, 24–29.
Xue, X., Guo, J., Han, B.S., Sun, Q.W., Liu, L.C., 2009. The effect of climate warming and permafrost thaw on sandy land in the Qinghai-Tibetan Plateau. Geomorphology 108, 182–190.
Yan, C.Z., Song, X., Zhou, Y.M., Duan, H.C., Li, S., 2009. Assessment of aeolian desertification trends from 1975's to 2005's in the watershed of the Longyangxia Reservoir in the upper reaches of China's Yellow River. Geomorphology 112, 205–211.
Zhang, Y., Ning, D., Smil, V., 1996. An estimate of economic loss for desertification in China. China Population, Resources and Environment 6, 45–49.
Zhang, Y.Z., Chen, Z.Y., Zhu, B.Q., Luo, X.Y., Guan, Y.N., Guo, S., Nie, Y.P., 2008. Land desertification monitoring and assessment in Yulin of Northwest China using remote sensing and geographic information systems (GIS). Environmental Monitoring and Assessment 147, 327–337.
Zhao, H.L., Zhang, T.H., Chang, X.L., 1999. Cluster analysis on change laws of the vegetation under different grazing densities in Horqin sandy pasture. Journal of Desert Research 19, 40–44.
Zhao, J., Wei, C.J., Huang, L.F., 2001. Research methods of land use changes and their applications in Hainan Island. Geographical Research 20 (6), 723–730.
Zhu, J.H., Li, J.S., 2002. A study on desertification of west Jilin Province based on remote sensing and GIS techniques. Chinese Geographical Science 12, 73–79.
Zhu, Z.D., Liu, S., 1984. Concept of desertification and the differentiation of its development. Journal of Desert Research 4, 2–8.